**Showcasing research from the groups of Prof. André Bardow, Prof. Jürgen Klankermayer, Prof. Walter Leitner, Prof. Alexander Mitsos and Prof. Stefan Pischinger at RWTH Aachen University.**

Cleaner production of cleaner fuels: wind-to-wheel – environmental assessment of CO_2-based oxymethylene ether as a drop-in fuel

This study presents a comprehensive environmental Life Cycle Assessment for a potential diesel fuel blend with CO_2-based oxymethylene ethers (OME). The well-to-wheel analysis reveals the shortest oxymethylene ether, dimethoxymethane (OME_1), as almost carbon-neutral blending component with substantially reduced NOx and soot emissions during combustion. These environmental benefits are enabled by the integration of renewable energy into the fuel value-chain.
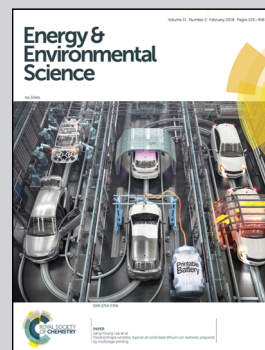
ROYAL SOCIETY OF CHEMISTRY

rsc.li/ees

Check for updates

Cleaner production of cleaner fuels: wind-to-wheel – environmental assessment of CO_2-based oxymethylene ether as a drop-in fuel†

Sarah Deutz, [ID] [a] Dominik Bongartz, [ID] [b] Benedikt Heuser, [ID] [c] Arne Kätelhön, [ID] [a]
Luisa Schulze Langenhorst, [ID] [b] Ahmad Omari, [ID] [c] Marius Walters, [ID] [c]
Jürgen Klankermayer, [ID] [d] Walter Leitner, [ID] [de] Alexander Mitsos, [ID] [b]
Stefan Pischinger [ID] [c] and André Bardow [ID] *[a]

The combustion of fossil fuels within the transportation sector is a key driver of global warming (GW) and leads to harmful emissions of nitrogen oxides (NOx) and particulates (soot). To reduce these negative impacts of the transportation sector, synthetic fuels are currently being developed, which are produced from renewable energy stored *via* catalytic conversion of hydrogen (H_2) and carbon dioxide (CO_2). A promising class of synthetic fuels are oxymethylene ethers (OMEs). This study conducts a prospective environmental assessment of an OME-based fuel using Life Cycle Assessment (LCA). We investigate an OME_1-diesel-blend (OME_1-blend), where OME_1 replaces 24 mass% of diesel fuel. Such an OME_1-blend could be a first step towards an OME transition. For the production of OME_1 from CO_2-based methanol, we consider both the established route *via* condensation with formaldehyde and a novel direct pathway based on catalytic combination with CO_2 and hydrogen. To close the carbon loop, CO_2 supply *via* biogas and direct air capture is considered. In a best-case scenario, hydrogen is produced by water electrolysis using electricity from wind power in the European Union as an input. The direct pathway reduces the required process steps from three to two and is shown to allow for an improved utilization of the energy provided by hydrogen: the exergy efficiency is increased from 74% to 86%. For combustion, we conducted experiments in a single cylinder engine to determine the full spectrum of engine-related emissions. The engine data provide the input for simulations of the cumulative raw emissions over the Worldwide Harmonized Light Vehicles Test Procedures (WLTP) cycle for a mid-size passenger vehicle. Our well-to-wheel LCA shows that OME_1 has the potential to serve as an almost carbon-neutral blending component: replacing 24 mass% of diesel by OME_1 could reduce the GW impact by 22% and the emissions of NOx and soot even by 43% and 75%, respectively. The key to achieving these benefits is the integration of renewable energy in hydrogen production. The cumulative energy demand (CED) over the life cycle is doubled compared to fossil diesel. With sufficient renewable electricity available, OME_1-blends may serve as a promising first step towards a more sustainable transportation sector.

Broader context

In recent years, environmental challenges such as global warming (GW), air pollution and resource depletion have increased the need for the application of sustainable technologies in the transportation sector. The transportation sector is central to achieving environmental targets since it contributes about 23% to the global carbon (CO_2) emissions. The environmental impact is mainly caused by both the production and the combustion of fossil fuels. Reducing these impacts requires a shift away from fossil fuels towards more sustainable energy carriers. For this purpose, synthetic fuels are developed by reacting carbon dioxide with hydrogen obtained from water electrolysis. Thereby, renewable energy is integrated into the transportation sector. A recent class of synthetic fuels are oxymethylene ethers (OMEs). They are accessible from CO_2 and H_2 *via* methanol as a molecular pivot. In addition, OMEs allow a substantially cleaner combustion in terms of nitrogen oxides (NOx) and soot emissions compared to fossil diesel. OMEs can be distributed using existing infrastructure and combusted in existing engines with minor adjustments (*e.g.* sealing and fuel line materials, and minimal adaptations in the engine control unit to account for a lower heating value). Therefore, they could potentially serve as a drop-in fuel. To quantify the potential benefits from OME fuels, a comprehensive environmental assessment is mandatory to evaluate the environmental performance from well-to-wheel – or more specifically from wind-to-wheel.

[a] *Institute of Technical Thermodynamics, RWTH Aachen University, Schinkelstraße 8, 52062 Aachen, Germany. E-mail: andre.bardow@ltt.rwth-aachen.de*
[b] *Process Systems Engineering (AVT.SVT), RWTH Aachen University, Forckenbeckstraße 51, 52074 Aachen, Germany*
[c] *Institute for Combustion Engines, RWTH Aachen University, Forckenbeckstraße 4, 52074 Aachen, Germany*
[d] *Institute of Technical and Macromolecular Chemistry, RWTH Aachen University, Worringerweg 1, 52074 Aachen, Germany*
[e] *Max-Planck-Institute for Chemical Energy Conversion, Stiftstraße 34-36, 45470 Mülheim a.d. Ruhr, Germany*
† Electronic supplementary information (ESI) available. See DOI: 10.1039/c7ee01657c

1 Introduction

Today, the transportation sector almost exclusively depends on fossil fuels. The combustion of fossil fuels within the transportation sector is a major driver of global warming and also a source of local pollutant emissions especially of nitrogen oxides (NOx) and soot.[1] Both NOx and soot emissions are harmful for human health, and NOx further contributes to acidification, eutrophication and ozone depletion.[2] In Europe, nearly 23% of energy-related greenhouse gas emissions[3] and 46% of the NOx emissions[4] are caused by the transportation sector. To substantially reduce these negative impacts of the transportation sector, a shift away from fossil fuels towards renewable energy carriers should urgently be considered.

Renewable energy can be integrated into the transportation sector by its conversion into the chemical energy carrier hydrogen (H_2) through water electrolysis and its catalytic conversion with carbon dioxide (CO_2) to liquid fuels.[5–14] CO_2 can be captured after combustion, from biogenic sources or even directly from the air.[15] By this means, synthetic fuels can contribute to closing the carbon cycle, and potentially become carbon neutral. At the same time, the transition from fossil to renewable feedstocks opens the potential for tailormade fuels with improved properties such as high combustion efficiencies and low pollutant emissions over the whole value chain.[16] The most studied examples of CO_2-based fuels are methane,[11,14] methanol,[10,14,17–19] dimethyl ether (DME),[10,14,17,20] and Fischer–Tropsch-fuels.[13,21]

Recently, a promising class of novel synthetic fuels is receiving attention: oxymethylene ethers (OMEs) also known as poly-(oxymethylene) dimethyl ethers.[22–29] OMEs are liquid fuels that can be combusted in conventional diesel engines and distributed using existing infrastructure. Hence, OMEs have the potential to be used immediately as drop-in fuels, which means that OMEs could directly replace fossil diesel fuel. OMEs can be produced with different chain lengths; while medium-chain OMEs can directly substitute diesel, OME_1 (also known as methylal or dimethoxymethane) should be blended with fossil diesel. Pure OME_1 has a low boiling point (42 °C) and high vapor pressure which would lead to storage and handling requirements similar to gaseous fuel. However, when blending OME_1 into diesel the OME_1-blend can be handled similar to Gasoline (*i.e.*, higher volatility, lower viscosity and a low flashpoint compared to diesel fuel). Hence, in contrast to pure OME_1, OME_1-blends are expected to be compatible with the existing fuel distribution infrastructure with minor adjustments. Depending on the amount of OME_1 blended in fossil diesel, minor modifications are expected to be necessary: the sealing material and fuel line material might be replaced. In the engine, the control unit might need minor adaption to determine injector opening duration. Overall, such OME_1-blends may thus be the first step towards a transition to OME fuels.

Compared to fossil diesel, OME fuels have a higher oxygen content, leading to significantly lower soot emissions during combustion.[25,27] The inherent reduction of soot formation enables further reduction of NOx emissions by increasing the rate of exhaust gas recirculation (EGR). With fossil diesel fuel, increased EGR rates would reduce the oxygen concentration in the combustion chamber, thereby producing high amounts of soot. In contrast, the lower tendency for soot formation of OME fuels allows for more favorable combustion conditions with both reduced soot and NOx emissions.[25,27] Despite the promising prospects of OME fuels, a comprehensive environmental evaluation of OME fuels is currently missing.
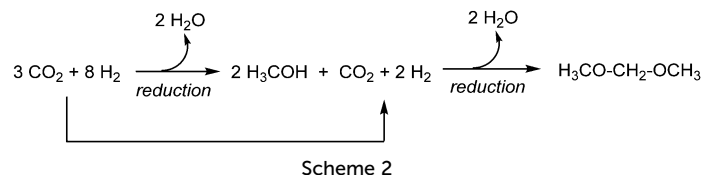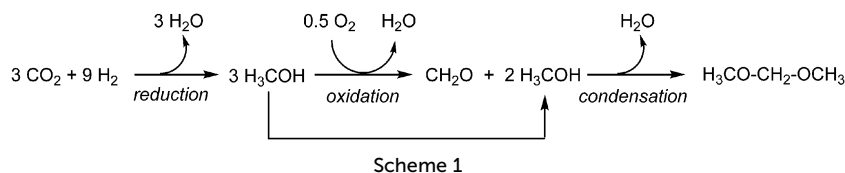
Herein, we conduct such a comprehensive environmental evaluation using Life Cycle Assessment (LCA). We study OME_1 produced from H_2 and CO_2 where H_2 is obtained from water electrolysis and CO_2 is captured from air or from a biogas plant and combusted in a 35 vol% blend with diesel fuel. The 35 vol% of OME_1 replaces 24 mass% of fossil diesel due to the lower heating value of OME_1. Consequently, the volumetric fuel consumption increases by approximately 20% compared to fossil diesel assuming equal energetic efficiencies. The environmental impacts of the OME_1-blend are benchmarked with fossil diesel fuels over the full life cycle from production to combustion in an engine. For the production of OME_1, we consider two alternative routes starting from methanol as the common intermediate. In both routes, methanol is obtained from CO_2 *via* catalytic reduction with hydrogen (H_2) that is produced by electrolysis of water, which enables the use of renewable energy. In the first route (Scheme 1), OME_1 is produced *via* a condensation reaction from methanol and formaldehyde (FA).[28,30,31] However, since production of formaldehyde first involves an oxidative step, the overall route is redox-inefficient. As a second route (Scheme 2), we consider a purely reductive approach to OME_1 which was recently demonstrated based on the direct transformation of methanol with CO_2/H_2 to catalytically generate the central CH_2-unit of the OME molecule.[32,33]

To characterize the combustion of the OME_1-blend, we perform tests in a single cylinder engine. These engine tests provide input data for simulations of a full driving cycle. Based on the engine tests and the full driving cycle simulations, we determine the full spectrum of raw combustion emissions.

While previous LCA studies on transportation examine fossil fuels from "Well-to-Wheel",[34–36] this work changes the focus towards renewable energies, and assesses the potential environmental impacts of OME fuels from "Wind-to-Wheel". Correspondingly, our best-case scenario assumes electricity from wind power in the European Union as input for water electrolysis to produce hydrogen. The worst-case scenario employs the expected European electricity grid mix 2020, and a sensitivity analysis is carried out.

This paper is structured as following the steps of a life-cycle assessment study according to ISO 14040/14044:[37,38] in Section 2, we define the goal and scope of the LCA. Section 3 provides the life cycle inventory with a detailed discussion of the technical characteristics of the life cycle of OME_1-blends, and discusses the data collection. In Section 4, the life cycle impact assessment is performed and the results of the study are shown and discussed, before conclusions are drawn in Section 5.

$$3\,CO_2 + 9\,H_2 \xrightarrow[\text{reduction}]{3\,H_2O} 3\,H_3COH \xrightarrow[\text{oxidation}]{0.5\,O_2 \quad H_2O} CH_2O + 2\,H_3COH \xrightarrow[\text{condensation}]{H_2O} H_3CO\text{-}CH_2\text{-}OCH_3$$

Scheme 1

$$3\,CO_2 + 8\,H_2 \xrightarrow[\text{reduction}]{2\,H_2O} 2\,H_3COH + CO_2 + 2\,H_2 \xrightarrow[\text{reduction}]{2\,H_2O} H_3CO\text{-}CH_2\text{-}OCH_3$$

Scheme 2

2 Goal and scope of the life cycle assessment of OME$_1$-blends

LCA is a comprehensive environmental assessment method for products and services.[37–40] The LCA method generally takes into account the entire life cycle, from the extraction of raw materials to final disposal of waste. Throughout the life cycle, all flows of energy and material that are exchanged with the environment are collected and interpreted with regard to their environmental impacts. Various impact categories are usually considered such as global warming (GW) and acidification. A detailed description of the LCA methodology is provided by ISO 14040/14044.[37,38] In addition, Carbon Capture and Utilization (CCU)-specific LCA guidance is provided by von der Assen et al.[39,40] In the following, we discuss the goal and scope of the LCA of the OME$_1$-blend.

Goal

In the environmental assessment of the OME$_1$-blend, we pursue two goals: the primary goal is to determine the potential reduction of environmental impacts by OME$_1$-blends compared to fossil diesel fuel. The secondary goal is to compare the conventional OME$_1$ production process based on methanol and formaldehyde (FA-route)[28,30,31] to a novel production route in which OME$_1$ is catalytically formed from methanol and CO$_2$ and H$_2$ directly (direct-route).[33] In the overall analysis of both processes, methanol is assumed to be produced from CO$_2$ and H$_2$. In the FA route, a part of the methanol has to be oxidized to formaldehyde in an additional process unit, followed by the condensation step to yield OME$_1$. In the direct route, the central CH$_2$-unit of OME$_1$ is formed reductively from CO$_2$/H$_2$ in the presence of methanol. Thus, the direct route is "direct" in the sense that it avoids the additional oxidative conversion step from methanol to formaldehyde.

System boundaries

Compared to fossil diesel, OME$_1$-blends are produced via different production pathways and show a different emission profile during combustion. Consequently, the comparative environmental assessment of OME$_1$-blends and fossil diesel needs to include both the production of the fuel and its use in the engine. The chosen system boundaries thus encompass the so-called cradle-to-grave approach covering all stages of the life cycle. The construction of the vehicle is not considered since the OME$_1$-blends are used as drop-in fuels in current vehicles and engine systems. Thus, the construction of the vehicle is assumed equal for both fuels.

To compare alternative OME$_1$ production routes, the combustion of the OME$_1$-blend within the engine can be neglected, because OME$_1$ produced via the alternative production routes is chemically identical. Therefore, no differences in environmental impacts during combustion occur. Consequently, to compare the alternative OME$_1$ production routes, we follow a cradle-to-gate approach covering only the production stages of OME$_1$. Since electricity is the major input for fuel production, we vary the electricity sources to study the potential impacts.

Functional unit

In LCA, products are compared based on a so-called functional unit, which quantifies the function of the investigated product systems and serves as a basis for comparison. To compare the environmental impacts of OME$_1$-blends to fossil diesel, we use the functional unit "1 km driving a passenger vehicle". Hence, this functional unit captures the ultimate purpose: the provision of transportation.

For the ease of interpretation, the alternative OME$_1$ production routes are compared to each other based on the functional unit "1 kg OME$_1$" since the rest of the life cycle would be identical such that cradle-to-gate boundaries suffice. This functional unit thus analyzes how to best produce OME$_1$ – and is independent from its potential use as a fuel or e.g. as a chemical.

Environmental indicators

The main motivation of using OME fuels is the reduction of environmental impacts and emissions. Our assessment therefore focuses on the following environmental indicators: (i) the environmental impact category global warming (GW), (ii) emissions of NOx, (iii) emissions of soot, and (iv) the cumulative energy demand (CED), which specifies the cumulated amount of both primary fossil and renewable energy used. GW and fossil CED capture issues of major global concern: climate change and the depletion of fossil resources. The GW impact is

This journal is © The Royal Society of Chemistry 2018

Energy Environ. Sci., 2018, 11, 331–343 | 333

determined according to IPCC following the Recommendations for Life Cycle Impact Assessment by the European Commission.[41] The environmental indicator CED is calculated based on Fischknecht *et al.*[42] Emissions of NOx and soot are important local emissions of current combustion engines which are therefore subject to increasingly stringent regulations. NOx and soot emissions due to combustion are determined directly from our experiments and the subsequent cycle simulations.

Exergy analysis

To obtain a deeper insight into the fundamental differences between the conventional FA route and the novel direct route to OME$_1$, we further conduct an exergy analysis for the production. Exergy measures the maximum work that can be produced and is a thermodynamically consistent way to compare different forms of energy such as heat, electricity and chemical energy (for details see the ESI,† Section S1 and Table S5). The exergy efficiency of a process route represents the share of exergy inputs that is incorporated into the fuel, and can be determined here by the following equation

$$\eta_{ex} = \frac{\dot{m}_{OME_1} e_{OME_1}}{\sum \dot{W}_i + \sum \dot{E}_{Q_i} + \dot{m}_{H_2} e_{H_2} + \dot{m}_{CO_2} e_{CO_2}}, \quad (1)$$

where $\dot{m}_{OME_1}$, $\dot{m}_{H_2}$, and $\dot{m}_{CO_2}$ represent the mass flows of OME$_1$, H$_2$ and CO$_2$, respectively. e_{OME_1}, e_{H_2}, and e_{CO_2} are the specific exergies of OME$_1$, H$_2$ and CO$_2$. $\dot{W}_i$ and $\dot{E}_{Q_i}$ denote the electricity demand and exergy of the heat demand, respectively (for details on the calculations, see the ESI,† Section S1).

Determination of environmental impact reductions

The environmental impact reductions due to the substitution of fossil diesel through OME$_1$-blends are calculated for each environmental indicator EI:

$$EI_{reduction} = EI_{diesel} - EI_{blend}, \quad (2)$$

where EI_{diesel} and EI_{blend} represent the environmental indicator result for fossil diesel and for the OME$_1$-blend, respectively.

The resulting environmental impact reductions, however, refer to the entire blend (OME$_1$ and fossil diesel), and thus do not isolate the contribution of OME$_1$ as a blending component. To determine this contribution, we further introduce the blending effectiveness factor (BEF):

$$BEF = \frac{EI_{reduction}}{EI_{diesel} w_{diesel_{replaced}}} = \frac{\% \text{ of environmental impacts reduced}}{\% \text{ of diesel replaced}}. \quad (3)$$

This factor quantifies the percentage of environmental impact reduction compared to the mass percentage $w_{diesel_{replaced}}$ of replaced diesel. An interpretation of the blending effectiveness factor BEF is given in Table 1.

3 Life cycle and life cycle inventory for the OME$_1$-blends

In the life cycle inventory phase, mass and energy contents are collected and analyzed for all flows entering and leaving the

Table 1 The interpretation of the blending effectiveness factor (BEF), eqn (3)

BEF	Regime	Effect of the blending component
BEF < 0	Harmful blending	Blend worse than pure diesel
0 < BEF < 1	Blending regime	Blending component reduces overall impacts but adds some impacts of its own
BEF = 1	Ideal blending	Blending component reduces overall impact proportional to the amount of diesel replaced, *i.e.*, blending component does not add any own impacts
BEF > 1	Synergistic blending	Blending component acts synergistically: it does not only avoid any own impacts but reduces diesel impact

life-cycle of the OME$_1$-blend and of the reference process based on fossil diesel. The production phase is discussed in the following Section 3.1. First, the two alternative production processes are described. Subsequently, scenarios for the supply of all inputs are specified. In Section 3.2, the combustion of OME$_1$-blends in the engine is analyzed. Fig. 1 provides an overview of the individual life cycle stages of the OME$_1$-blend.

3.1 OME$_1$ production

For the production process of OME$_1$, we consider two alternative OME$_1$ synthesis pathways: the conventional production *via* the condensation of methanol and formaldehyde[30,31] and a new catalytic transformation allowing the direct synthesis of OME1 from methanol, CO$_2$ and H$_2$.[32,33]

FA route. In the FA route, OME$_1$ is formed in an acid-catalyzed reaction of methanol and formaldehyde (*cf.* Fig. 1).[30] Methanol is produced based on CO$_2$ and H$_2$, and formaldehyde is synthesized from CO$_2$-based methanol through a process based on combined dehydrogenation and partial oxidation over a silver catalyst (see Section S1 in the ESI†). The hydrogen formed from the dehydrogenation is burned to generate additional heat for reuse in the OME$_1$ production step. Thus, the cumulative material and energy flows are similar to the integrated partial oxidation of the so-called Formox process, which is therefore not treated separately. These two processes represent the most widely applied technology for formaldehyde production allowing for a rapid integration into existing value chains. The data collection for the FA route has been carried out based on literature sources[30,31,43–45] for the formation of methanol, formaldehyde, and OME$_1$. These separate production steps have been combined through mass balances and heat integration. Heat integration assumes that all process steps are carried out at the same site. The resulting overall life cycle inventory data for this route is summarized in Table 2. Details on the underlying processes can be found in the ESI,† Section S1.

Direct route. In the direct route, OME$_1$ is directly produced from methanol, CO$_2$, and H$_2$ (*cf.* Fig. 1). Thereby, the formaldehyde-unit is generated by catalytic reduction of carbon dioxide with hydrogen and directly trapped with methanol in a one-reactor system.[32,33] Thus, the need for the oxidative step of
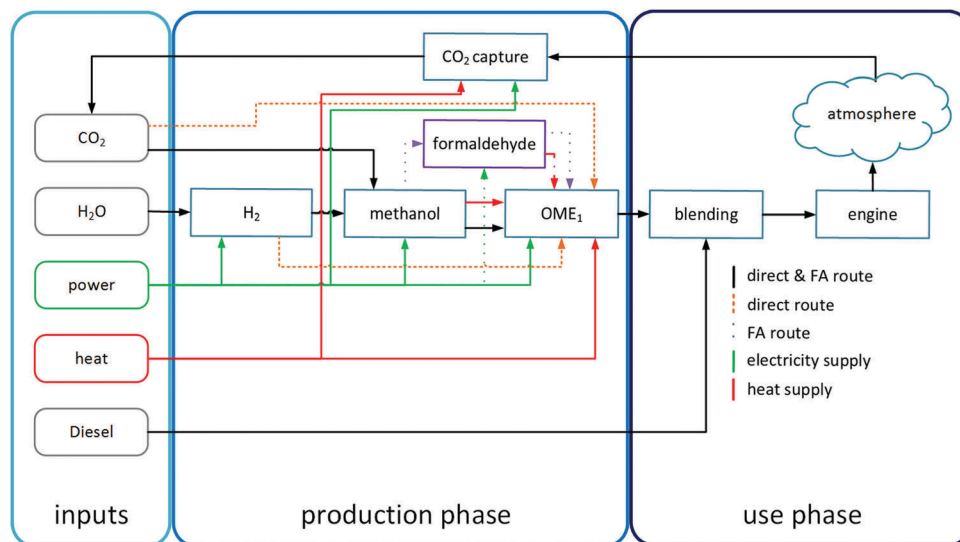
Fig. 1 The flowchart of the OME_1-blend life cycle is shown for the direct and the FA synthesis pathway. The rounded boxes present the input flows. The input CO_2 is obtained from recycling as described in the text. The rectangular boxes show the single process steps. The solid lines apply to both production routes. The dashed orange lines correspond to the direct route. The dotted purple lines belong to the FA route. The green lines represent the power supply, while the red lines show the heat supply.

formaldehyde formation is eliminated. This reduces the overall hydrogen consumption. The demand for feedstock supply of CO_2 is also reduced compared to the FA route since less CO_2 is lost by direct emissions in the process. Since the feasibility of the direct route has only recently been demonstrated experimentally,[32,33] a detailed process design is not yet available. We therefore conduct a simplified analysis to estimate the demand of reactants, work, and heat. Even though a detailed economic evaluation is beyond the scope of the present work, we expect the direct route to be economically beneficial compared to the FA route. The direct route requires one reactor less and possibly also less heat exchangers and separation equipment, while the size of the methanol plant can be reduced simultaneously. Furthermore, the direct route consumes less renewable hydrogen, which is typically the major cost driver in power-to-fuel applications.[45]

In this simplified analysis, the mass balance of the direct OME_1 production from methanol, CO_2 and H_2 is assumed to correspond to the reaction stoichiometry. Therefore, the assumed mass flows represent a best-case scenario for the direct route. Based on this assumption, the overall yield of OME_1 with respect to CO_2 increases to 98% compared to 92% in the FA route, since losses due to oxidation in formaldehyde production are eliminated. For product separation, the energy demand has been assessed based on the phase diagrams of the mixtures involved, as well as on calculations using pinch-based process models.[46] These assessments have shown that no additional azeotropes exist beside the ones occurring in the FA process for OME_1 production. Such azeotropes would increase the heat demand significantly. The pinch-based process models determine similar minimal heat demands for the FA route and the direct route (for all details see the ESI,† Section S1). We therefore assume the same heat demand for

separation for both routes and use the value from the FA route. A more rigorous analysis is required once detailed process concepts have been developed. The overall heat demand of the direct route, however, is higher since less waste heat is available within the process chain for use in OME_1 production because of the absence of the FA production process. In contrast to the FA route, H_2 is pressurized from the pressure level at which it is provided at 75 bar to 80 bar in the direct route. For the electricity demand of the direct route, we therefore assume the amount of electricity needed for pressurization in addition to the amount of electricity consumed in the FA route. This calculation is conservative since the reactor pressure has not been optimized for the direct route yet, and it can be expected that improved catalysts and reactor concepts will allow for the use of lower pressures in an actual process. Overall, the sensitivity to the pressure increase for the direct route is low. Life cycle inventory data for the production of OME_1 via the direct route is also summarized in Table 2. A more detailed description of the technical characteristics of the direct route is provided in the ESI,† Section S1.

Table 2 Life cycle inventory data for the formaldehyde (FA) route and the direct route for the production of OME_1 from H_2 and CO_2 via methanol. Negative values denote outputs, while positive values are inputs

Flow	FA route	Direct route
Masses [kg kg_{OME1}^{-1}]		
Feedstock H_2	+0.26	+0.22
Feedstock CO_2	+1.89	+1.77
Product OME_1	−1.00	−1.00
Direct CO_2 emissions	−0.15	−0.034
Energies [MJ kg_{OME1}^{-1}]		
Electricity	+0.42	+0.23
Heat at 385 K	+4.56	+7.64

This journal is © The Royal Society of Chemistry 2018

Energy Environ. Sci., 2018, 11, 331–343 | 335

Supply of H_2, CO_2, and utilities. For the supply of H_2, we consider a polymer electrolyte membrane (PEM) electrolysis at 75 bar with an electricity demand of 52 kW h per kg H_2[47] corresponding to a future unit. Today, a state of the art PEM cell requires 55 kW h per kg H_2 at atmospheric pressure. PEM electrolysis at higher pressure stages offers the possibility of delivering directly compressed H_2, which is energetically favorable if compressed H_2 is needed at the following process steps. The life cycle inventory data for the production of the electrolyzer are based on data from the LCA database Ecoinvent.[48] These data refer to PEM stacks with an electric output of 2 kW. Furthermore, we assume a life time of 15 years (80 000 h operation).[48] PEM electrolysis is beneficial for the integration of renewable electricity, because it allows dynamic operation using fluctuating electricity supplies such as wind electricity.[49–51] Details of the considered electrolyzer are summarized in Table S6 in the ESI.†

For the CO_2 supply, we consider two alternative sources: a biogas plant and direct air capture (DAC). The environmental impacts of both CO_2 sources are determined using a comparative LCA approach: we compare the scenario without CO_2 capture to the scenario in which CO_2 capture is installed.[15]

In the biogas plant, CO_2 is co-produced with concentrations of about 25–55% in methane.[52] If methane is fed into the natural gas grid, the CO_2 needs to be separated in any case. Therefore, the environmental impact for the separation process is attributed to methane. If CO_2 is not utilized as fuel, it is completely emitted to the atmosphere. Consequently, CO_2 capture avoids CO_2 emissions at the biogas plant without additional emissions for capture. Thus, such a biogas plant corresponds to an ideal CO_2 source.[15]

In the case of the DAC system, CO_2 is captured from ambient air with a concentration of about 400 ppm. Due to the low concentration of CO_2, more energy is required to separate the CO_2. In the case of the DAC system, the environmental impact of the separation process is ascribed to the captured CO_2, because only CO_2 is produced. Consequently, DAC represents the upper bound for emissions due to CO_2 supply, whereas the biogas plant specifies the lower bound. However, despite the higher energy demand, it is important to note that DAC allows a decentralized CO_2 supply, which can be environmentally beneficial in the case of very long transportation distances to a higher concentrated CO_2 source.[15] Such considerations are not further addressed in this work.

For both CO_2 sources, energy is also required for the compression of CO_2 to 100 bar for transportation. The supply of this energy causes environmental impacts[15] which are also taken into account.

For electricity supply, we consider the current electricity from wind power in the European Union as the lower bound for the GW impact, and the expected European grid mix in 2020 as the upper bound. In addition, various country-specific grid mixes and a forecasted European grid mix for 2050 are considered in a sensitivity analysis. The European grid mixes for 2020 and 2050 are based on a forecast by the European Commission.[53]

For the heat supply, we consider an electric heater and a natural gas boiler.[54]

Table 3 The scenarios for the supply of CO_2, electricity and heat

	CO_2	Electricity	Heat	Storage
Best-case	Biogas	Electricity from wind power in the European Union[54]	Electric heater[54]	—
Worst-case	Direct air capture[15]	European grid mix 2020[54]	Thermal energy from natural gas[54]	—
Sensitivity study		European grid mix 2050[54]		H_2 storage
		Grid mixes of European countries today[54]		Lithium ion battery

Considering the choices between alternative technologies for the supply of the inputs CO_2, electricity, and heat, we define a best- and a worst-case scenario in terms of GW impact. In the best-case scenario, each input is produced by the technology with the lowest GW impact, while the worst-case scenario leads to the highest environmental impact. Both scenarios are specified in Table 3.

In the best-case scenario, electricity is provided by wind power, which is an intermittent electricity source. To enable steady-state operation of the OME_1 production process, H_2- and electricity storage are required. For both scenarios, we simply assume 8000 full load hours annually. Thus, no storage is required for H_2 and electricity. Thereby, we can avoid the many assumptions required to specify storage and provide a best-case estimate. This estimate is tested in the sensitivity study, where we assume 2500 full load hours per year for the part-load operation[51] and include a pressure hydrogen storage to cover one week without intermittent renewable energies. For the construction of the H_2 storage, we only consider the steel demand according to Mori et al.[55] Due to the lack of data, we neglect the energy demand to produce the storage unit and the procurement of additional materials or equipment e.g. pumps, compressors, pipes etc. For electricity storage, we assume a lithium-ion battery with a life time of 6000 cycles[56] and an energy density of 120 W h kg^{-1}.[57] The life cycle inventory of the lithium ion battery production is based on measurements and is taken from LCA database Ecoinvent.[47] The battery pack includes 14 single cells and provides an electric power of 2.1 kW h.[47] For the anode and the cathode material, lithiated graphite (LiC_6) and lithium manganese dioxide ($LiMn_2O_4$) are used.[47] Details of the H_2 storage and the lithium ion battery are specified in Table S6 of the ESI,† Section S1.

The LCA data sources for all considered processes are summarized in Table S7 of the ESI,† Section S1.

Diesel. For the production of fossil diesel, we assume a European market mix for diesel based on the LCA database Thinkstep.[54] The market mix covers the entire supply chain from extraction over transportation and the refinery to the gas

336 | Energy Environ. Sci., 2018, **11**, 331–343

This journal is © The Royal Society of Chemistry 2018

station. The market mix includes conventional and unconventional production technologies from all delivering countries and country-specific crude oil mixes. For crude oil processing, country-specific technologies and supply chains are used. The share of biogenic components is 7.23 mass%. For the combustion experiments, we use conventional diesel from a filling station in accordance with EN950.

3.2 OME_1-blend combustion

The use phase of OME_1 consists of two steps: the blending with fossil diesel and the combustion of the blend in the engine. For blending, some of the authors recently examined several compositions of OME_1-blends with regard to emissions and combustion characteristics.[58] A favorable compromise between emission reduction and the deterioration of fuel properties like Cetane number and heating value has been found for the composition of 35/65 vol% OME_1/fossil diesel fuel blend, which is used for the experiments described in the following.

To characterize the engine-related raw emissions of the OME_1-blend, we conduct engine tests with a single cylinder engine using a global Design of Experiments (DOE) approach. In these tests, the speed and load range is varied to cover the complete Worldwide Harmonized Light Vehicles Test Procedure (WLTP) cycle. The WLTP is an upcoming procedure for vehicle certifications and has been designed to capture real-world driving scenarios and thus also real-world emissions better than the New European Driving Cycle (NEDC). The WLTP will replace the NEDC in Europe in September 2017. Specifications of the single cylinder research engine used for the DOE investigation are given in Table S8 in the ESI,† Section S2. Specifications of the emission measurement equipment are summarized in Table S9 and the calibration parameters varied in the DOE are given in Table S10 in the ESI,† Section S2. For each fuel, the DOE measurement campaign covered 40 load points and an average of 5 variations of calibration parameters per load point. Thus, 200 points where available for the subsequent creation of DOE-models.

From the measured data, global DOE models are created using the ETAS ASCMO software.[59] The software uses a multiple Gaussian regression analysis procedure to fit the measured data (emissions, fuel consumption, *etc.*) to a corresponding model. The input parameters are all varied engine calibration parameters as listed in Table S9 in Section 2 of the ESI.† With the generated models, the ETAS ACMO optimizer tool was used to obtain an optimal set of calibration maps for predefined settings. An optimal trade-off between emissions, low fuel consumption and combustion sound level were set as optimization goals.

Then, with the optimized engine calibration, emission maps were created from the DOE-models. These maps were subsequently used to simulate the cumulative raw emissions for the WLTP cycle. The resulting raw emissions represent the exhaust gas from the engine before any potential exhaust gas aftertreatment system. For the engine calibration, 3 scenarios were considered:

• Diesel with a calibration adapted according to the listed optimization criteria (diesel baseline)

• 35 vol% OME_1-blend with an engine calibration equal to diesel, with EGR adapted to meet NOx levels equal to diesel (NOx eq. to diesel)

• 35 vol% OME_1-blend with a calibration optimized for low emissions (optimized)

The cycle simulation assumed a D-segment passenger car (mid-size vehicle) with a representative road-load curve. Influences of thermal and transient effects (*i.e.* coolant heat-up and turbocharger response times) where not regarded in the simulation. For upcoming vehicle technologies, these effects may cause increased emissions by up to 5%. However, capturing these phenomena accurately does not justify the large additional effort needed on the test bench and thus was not performed in this work. The settings for the cycle simulation and the exhaust aftertreatment system are summarized in Table S10 in the ESI,† Section S2.

To determine the tailpipe emissions of a vehicle, the exhaust gas aftertreatment needs to be taken into account. For the exhaust aftertreatment system, several strategies are available. The diesel oxidation catalyst (DOC) oxidizes carbon monoxide (CO) and hydrocarbons (HC) to CO_2 and water.[60] Selective catalytic reduction (SCR) reduces the NOx emissions by reduction with ammonia to diatomic nitrogen.[60] Furthermore, diesel vehicles mostly use a diesel particulate filter (DPF) to reduce the soot emissions produced during the diffusive combustion of diesel fuel.[60] Nevertheless, in our further assessment, we report the cumulative raw emissions since they can be directly compared without considering the design and configuration of the exhaust gas aftertreatment system. Still, we also estimate the emission after the exhaust gas aftertreatment system below.

4 Environmental impacts of OME_1-blends

Based on the life-cycle inventory data collected in Section 3, the life cycle impact assessment (LCIA) can be performed and the result can be interpreted as the final phase of the LCA study. Life cycle impact assessment characterizes all flows entering or leaving the life cycle of the OME_1-blend and the reference process fossil diesel with regard to their effects on the considered environmental impact categories. In the following, the results of the environmental assessment are presented and discussed along the OME_1 life cycle. In the following Section 4.1, we focus on the production phase, and compare the environmental impacts of the two alternative OME_1 production routes. In Section 4.2, we continue with the use phase in the car, and present the emissions due to the combustion of the OME_1-blend over the WLTP cycle. In Section 4.3, we combine the assessments of the production and use phase to determine life cycle environmental impacts of the OME_1-blend compared to fossil diesel. A sensitivity analysis is performed in Section 4.4.

4.1 From cradle-to-gate: production of OME_1

Fig. 2 shows the GW impacts of OME_1 production based on the FA and the direct route. The GW impacts are determined for the
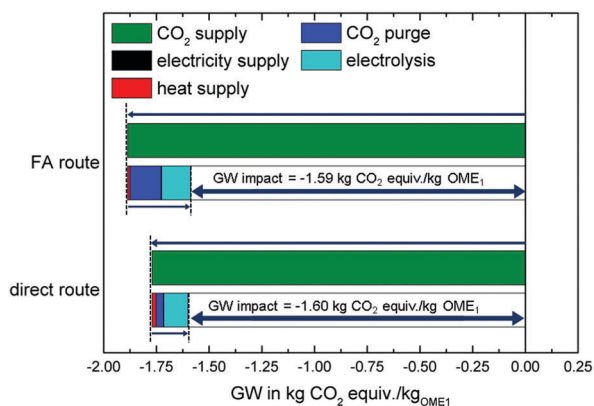
Fig. 2 Global warming (GW) impact from cradle-to-gate for the direct route and the FA route of OME_1 for the best-case scenario. The green bars denote the negative GW impact of the CO_2 supply captured from a biogas plant and thus avoiding emissions. The black, red, blue and cyan bars represent the positive GW impacts from the production of OME_1. The dark blue arrows represent the resulting total GW impact which is negative for both production routes.

Fig. 3 Sankey diagram showing exergy flows in (a) the FA and (b) the direct route.

best-case scenario (*cf.* Table 3) to show the potential lower bound of emissions due to OME_1 production.

Both routes have negative cradle-to-gate emissions for producing OME_1. This is due to the negative impacts of the CO_2 supply which assumes that emissions at the biogas plant are avoided (*cf.* Table 3). Negative cradle-to-gate emissions are required to reach carbon-neutrality over the full life cycle since CO_2 will be released from gate-to-grave in the combustion.

The GW impact results in the studied best-case scenario are very close and can be considered equal taking into account uncertainties. The FA route uses more CO_2 than the direct route reducing the GW impact due to the negative impacts of the CO_2 supply. In addition, the FA route requires less heat, because of better opportunities for heat integration with the synthesis reactions of methanol and formaldehyde (if the sites are co-located). However, the FA route also has a higher CO_2 purge and a substantially higher H_2 demand. Due to the higher H_2 demand, the GW impact of the electrolysis is increased compared to the direct route. The GW impact of electrolysis includes the production of the electrolyzer, the provision of water and the electricity required during operation.

To analyze the thermodynamic efficiency and to find the bottlenecks of both production routes, an exergy analysis was conducted. Fig. 3 shows the flows of exergy in both production routes in a Sankey-Diagram. The width of the flows represents the amount of exergy of the flow. In the FA route (Fig. 3a), the formation of formaldehyde causes the largest exergy loss. In this step, methanol is partly lost to the tail gas of the absorption column (in the form of H_2, CO, and CO_2), and burned for steam generation. This exergy loss can be avoided in the direct route (Fig. 3b), where the separate oxidative formation of formaldehyde is not required. In addition, the direct route consumes less methanol. The exergy destruction in the FA process is mainly due to the combustion of the tail gas and heat transfer over finite temperature gaps. Additional exergy losses occur due
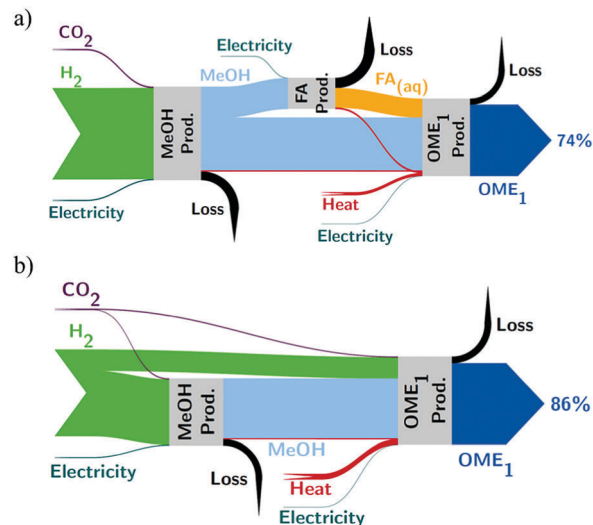
to residual heat in the exhaust gas stream and heat transferred to cooling water.

The reduced exergy losses in the direct route result in a higher exegetic efficiency: the direct route has an exegetic efficiency of 86%, while the FA route achieves an exegetic efficiency of 74%. The higher efficiency of the direct route indicates that the direct route is thermodynamically fundamentally advantageous and is able to direct more energetic value from the hydrogen input to the fuel.

4.2 From gate-to-grave: combustion of OME_1-blends

The results of the single cylinder engine investigations show that the combustion of the OME_1-blend leads to lower soot emissions compared to fossil diesel. Fig. 4 illustrates the relationship between the measured filter smoke number and
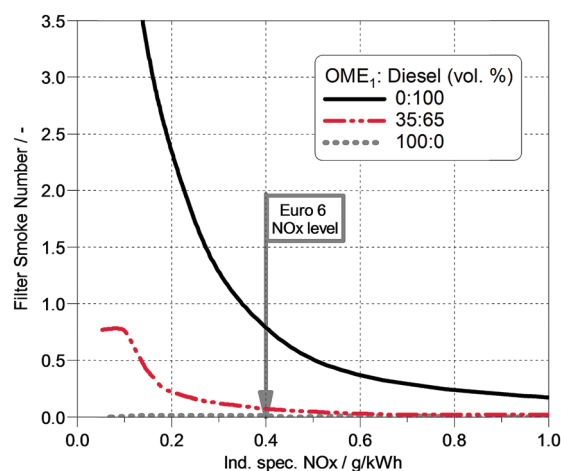

Fig. 4 Filter smoke number of diesel, 35% OME_1-diesel blend and pure OME_1 *versus* NOx emissions. The data are measured on a single cylinder engine at a mid-range load point: speed = 2280 min^{-1} and load = 9.4 bar indicated mean effective pressure.

the NOx emissions for diesel, 35% OME_1 blended with diesel and pure OME_1. The filter smoke number represents the blackness of a piece of filter paper after the exhaust gas flow has been led through at predefined system settings. The presented data were measured at a mid-range load point (speed = 2280 min^{-1} and load = 9.4 bar indicated mean effective pressure) using an AVL 415s smoke meter, which is the common device used for soot measurements in diesel engines. Fig. 4 clearly shows that blending of diesel with 35% OME_1 results in a strong reduction of soot emissions of up to ~90% over a wide range of NOx emission levels. Considering a common upper limit for the filter smoke number of 0.8, it can be seen from Fig. 4 that the NOx emissions for fossil diesel can be reduced to 0.4 g kW^{-1} h^{-1}. For the OME_1-blend, however, a further NOx reduction is possible, e.g. to 0.2 g kW^{-1} h^{-1} while still being far below the diesel filter smoke number 0.8. Thus, the inherent reduction of soot formation of the OME_1-blend enables further reduction of NOx emissions and avoids the soot-NOx trade-off of fossil diesel.

The improved emission behavior compared to fossil diesel is due to the fact that OMEs have a high amount of oxygen bound in the molecule (>42% by weight) and no direct molecular carbon–carbon bonds (CH_3–O–$(CH_2$–O$)_n$–CH_3), both of which contribute to a soot-free combustion of pure OME.[61] In addition, the lower boiling temperatures in comparison to diesel may contribute to an improved mixture formation, thereby further reducing the regions of oxygen-lack in the fuel spray. When blended with diesel, OME_1 acts as a soot-mitigating agent keeping the soot emissions of the blend significantly low as well.[25,58] The soot emissions are inherently reduced due to the molecular structure of OME_1, while the NOx emissions remain similar to fossil diesel combustion.[58] However, the extremely low soot emissions allow the exhaust gas recirculation rate (EGR) to be increased without a significant soot penalty, thereby providing the possibility for further NOx reduction.

The data from the single cylinder engine is used to calculate the cumulative raw emissions of CO_2, NOx and soot during the WLTP cycle for fossil diesel and the OME_1-blend (Fig. 5). For the OME_1-blend, two calibrations of the engine are considered as explained in Section 3.2: one calibration identical to the diesel baseline, with adaptation of EGR to meet equal NOx emissions compared to fossil diesel ("NOx eq. to diesel") and one calibration optimized for emissions ("optimized"). The calibration parameters considered in the optimization are given in Table S10 in Section S2 of the ESI.† The OME_1-blend retains the high efficiency of the diesel fuel and leads to similar tank-to-wheel emissions of CO_2 due to a similar carbon content (less than 0.2% decrease).

At the same time, the OME_1-blend has substantially lower soot emissions in both calibrations. The lowest soot emissions are achieved for the engine calibration, where the NOx emissions are equal to fossil diesel (reduction of 93%). In the optimized calibration, NOx emissions are reduced by about 50%, while the soot emissions are about 90% lower compared to diesel. The OME_1-blend leads to a substantially cleaner combustion in terms of NOx and soot.

The energy consumption, the cumulated raw emissions and the tail pipe emissions per km during the WLTP cycle are summarized in Table S11 in Section S2 in the ESI.†
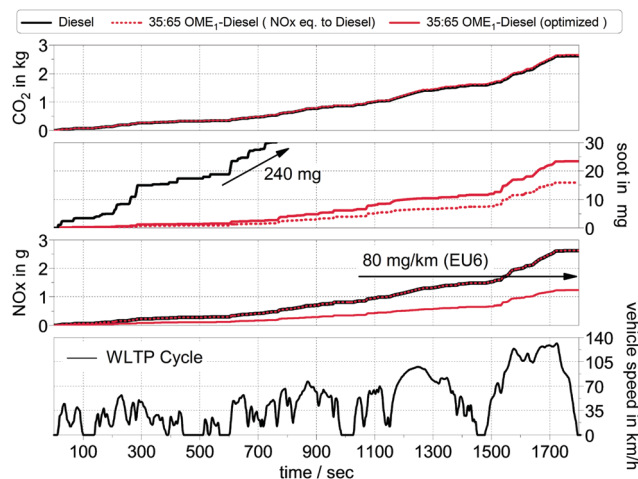

Fig. 5 Cumulative emissions of CO_2, NOx and soot simulated over the Worldwide Harmonized Light Vehicles Test Procedures (WLTP) cycle. For the OME_1-blend, two calibrations of the engine were used: the conventional diesel calibration (NOx eq. to diesel) and a variant optimized for low emissions, fuel consumption and combustion noise level (optimized).

The OME_1-blend retains the high energy efficiency of diesel and has the same energy consumption of 1.57 MJ km^{-1}. The tailpipe emissions represent the emissions after the exhaust gas aftertreatment system. For the aftertreatment system, the conversion efficiency was assumed to remain constant for each fuel.

For the OME_1-blend with the optimized engine calibration, the cumulative NOx raw emission level was found to be lower than the emission limit (EURO6, <80 mg km^{-1}).[62] This low NOx level could be even reduced by an exhaust gas aftertreatment system (cf. Table S11 in the ESI†). Alternatively, the NOx aftertreatment system could be simplified or even eliminated to achieve cost reductions. Nevertheless, this aspect was not in the focus of this work, but a detailed analysis of aftertreatment systems for OME fuels seems promising.

4.3 From cradle-to-grave: environmental impacts and blending effectiveness factor

Fig. 6a compares the LCA results for the OME_1-blend produced via the two production routes for the engine with optimized calibration to fossil diesel fuel over the entire life cycle. In the GW impact category, the OME_1-blend produced via both production routes reduces the impact by about 22% compared to fossil diesel. These GW impact reductions result from the production of OME_1 (see Section 4.1). During combustion, the OME_1-blend shows similar GW impacts as fossil diesel fuel (Section 4.2).

For NOx and soot emissions, in contrast, the combustion phase is most important. During combustion, OME_1-blends have shown substantially lower NOx and soot emissions than fossil diesel (Section 4.2). Over the entire life cycle, OME_1-blends have about 43% and 75% lower emissions of NOx and soot, respectively.

The fossil CED shows a very similar trend as the GW impacts: OME_1-blends reduce the fossil CED by about 22% in the best-case scenario. However, the demand of renewable CED increases for the OME_1-blend by factors of 19 and 22 for the direct and the FA route, respectively. A detailed discussion of the
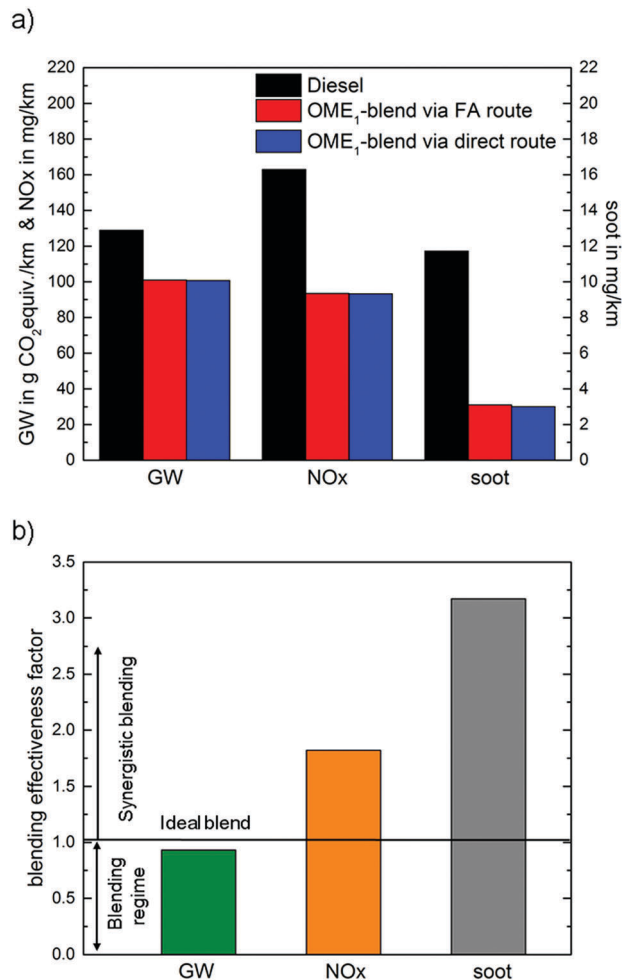
This journal is © The Royal Society of Chemistry 2018

Energy Environ. Sci., 2018, 11, 331–343 | 339

Fig. 6 (a) Cradle-to-grave analysis LCA results of the OME_1-blend with the optimized calibration and fossil diesel fuel for the best-case scenario. (b) Blending effectiveness factor (BEF) (eqn (3)) of the OME_1-blend for the global warming (GW) impact, and the emissions of NOx and soot for the best-case case scenario and the optimized engine calibration.

CED results is provided in the ESI,† Section S3 (Fig. S3). Overall, the combined fossil and renewable CED increases almost by a factor of 1.9 showing that a transition to synthetic fuels would require an expansion of the electricity sector to provide additional input for the transportation sector. In such a scenario, the production of synthetic fuels based on renewable energies, however, will compete with other power-to-X technologies.[12]

The contribution of OME_1 as a blending component can further be analyzed based on the blending effectiveness factor (BEF) introduced in Section 2 (see Fig. 6b). In the 35 vol% OME_1-blend, 24 mass% diesel fuel mass is replaced by OME_1. This reduces the GW impact by 22% leading to a blending efficiency of $BEF_{GW} = 22/24 = 0.93$. Hence, OME_1 is close to an ideal blending component (BEF = 1), which would introduce no environmental impacts of its own and only reduce the overall GW impact of fossil diesel fuel. The $BEF_{GW} = 0.93$ results from the substitution of fossil diesel by CO_2-based OME_1, which still adds some greenhouse gas emissions from the production and combustion of OME_1.

For NOx and soot emission reductions, the blending effectiveness factor BEFs are 1.8 and 3.2, respectively. Thus, replacing 24 mass% of diesel fuel by OME_1 reduces NOx emissions by $1.8 \times 24\% = 43\%$, and soot emissions even by $3.2 \times 24\% = 75\%$. As aforementioned, a BEF higher than 1 indicates that OME_1 reduces impacts stronger than due to simple substitution of an equivalent amount of fossil diesel fuel. In other words, OME_1 acts synergistically where a small amount has a beneficial effect that is larger than its share in the mixture. The reported BEFs are based on the studied OME_1-blend with 35 vol% of OME_1 and cannot simply be extrapolated due to nonlinear mixing behavior. For this purpose, further experiments are required but it is already apparent that OME fuels would significantly lower local emissions from combustion.

4.4 Sensitivity on OME_1 production scenarios

The LCA results presented in the previous sections were determined for the best-case scenario in terms of the GW impact (*cf.* Table 3). Consequently, these results represent the lower bound of the GW impact. In reality, however, the same inputs may be produced by other technologies resulting in a higher GW impact. To determine the potential range of the GW impact of the OME_1-blend, Fig. 7 shows the LCA results over the entire life cycle for both the best- and the worst-case scenario given in Table 3.

The GW impact of the OME_1-blend strongly depends on the supply chains. In the worst-case scenario, the GW impact is about twice as high as in the best-case scenario. Therefore, in the worst-case, the OME_1-blend is worse than fossil diesel fuel, and increases the GW impact by 31% and 33% for the blend produced by the direct and the FA route, respectively.

The major difference in GW impact is caused by the choice of electricity used for electrolysis to produce H_2. If electricity from the European grid as expected in 2020 is used, the GW impact of the H_2 supply is about a factor 38 higher than for electricity from wind.

Furthermore, the source for CO_2 influences the GW impact. If CO_2 is obtained from DAC, the GW impact of the OME_1-blend is higher than for CO_2 from a biogas plant due to the increased energy demand for the CO_2 separation. Still, the OME_1-blend would reduce the GW impact compared to fossil diesel fuel if CO_2 from air capture and wind electricity were employed. The heat supply also increases the GW impact of OME_1-blends if heat is produced from natural gas instead of wind power. The effect of the heat supply on the GW impact is larger for the direct route, because of the higher heat demand.

The potential range of the NOx emissions for the OME_1-blend is illustrated over the entire life cycle in Fig. S4 in the ESI,† Section S4. In the best-case scenario, OME_1-blends from both production routes reduce the NOx emissions, whereby the major impact results from the combustion and the supply of fossil diesel for blending. In the worst case-scenario, the OME_1-blend cannot compete with fossil diesel, and increases the NOx emissions by about 14% and 22% for the direct and the FA route, respectively. The electricity supply for electrolysis induces the highest impact of the NOx emissions.
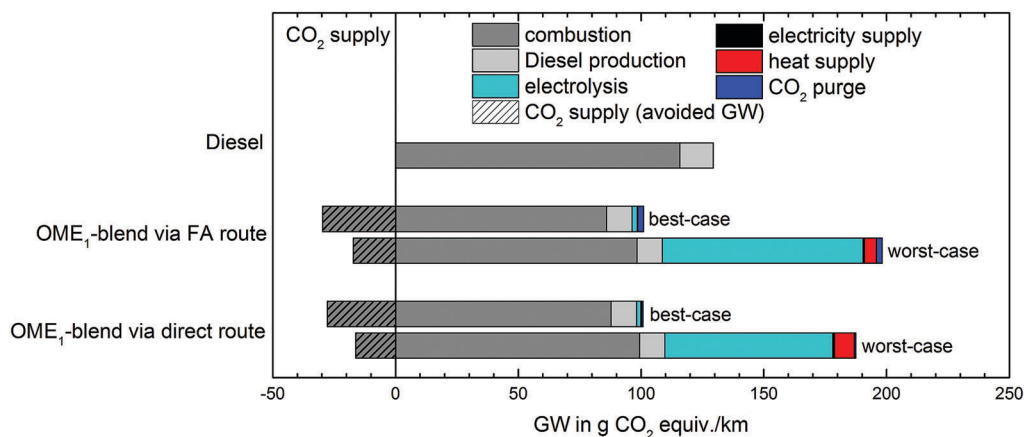
Fig. 7 Cradle-to-grave analysis of the global warming (GW) impact of the OME$_1$-blend and fossil diesel fuel for the best- and the worst-case scenario specified in Table 3.

The spectrum of potential soot emissions of the OME$_1$-blend can be found in Fig. S5 in the ESI,† Section S4. In contrast to the GW impacts and NOx emissions, the soot emissions are reduced in both the best-case and the worse-case scenario compared to fossil diesel. Even in the worst-case scenario, the soot emissions can be reduced by 43% and 36% for the direct and the FA blend. The electricity supply causes the major part of the soot emissions in the worst-case scenario.

Since the electricity source for electrolysis represents the most crucial factor for the GW impact and the emissions of NOx and soot, the effect of different electricity sources for the OME$_1$-blend (per km driven) is further illustrated for the GW impact in Fig. 8.

The GW impact of the OME$_1$-blend depends linearly on the GW impact of the electricity source. The dependence is stronger for the FA route than for the direct route due to the higher H$_2$ demand, which leads to a higher electricity demand. In Fig. 8, the crossings of the blue and red line with the black line represent the break-even points for GW impact reductions by the OME$_1$-blend. At these break-even points, the GW impact of the OME$_1$-blend is equal to the GW impact of the diesel fuel. The corresponding GW impact of the electricity supply specifies the maximum GW impact for which the OME$_1$-blend is still beneficial compared to diesel. For the FA route, the break-even point is 124 g CO$_2$ equiv. per kW h; for the direct route, it is 136 g CO$_2$ equiv. per kW h.

The results show that already today, it is possible to produce OME$_1$-blends with a lower GW impact than fossil diesel considering the grid electricity mix of various countries such as France, Sweden, Norway, and Iceland. The average European grid mix, however, is unlikely to deliver electricity with a sufficiently low GW impact even in the year 2050. Therefore, also in the future, it will be crucial to locate the OME production in places with an electricity mix with sufficiently large shares of renewable energy.

The influence of the different electricity sources on the NOx emissions is illustrated in Fig. S6 in the ESI,† Section S4. The correlation is similar to the one in Fig. 8, but the break-even points are reached such that electricity with higher impacts would still lead to an overall reduction. In this case,

reductions of NOx emissions can be achieved with the electricity mixes of Switzerland, France, Sweden, Norway, Iceland and the European wind electricity mix. The direct route also obtains reductions in NOx emissions with the European electricity grid mix 2050. For the soot emissions, the effect of the electricity mix is shown in Fig. S7 in the ESI,† Section S4. Due to the substantial reduction of soot emissions during combustion, reductions can be achieved with all considered electricity mixes.

These findings regarding the potential benefits of using grid electricity provide partial justification for the assumption of steady-state operation for the electrolysis in the previous section. Still, for the use of wind energy, storage would be required. Therefore, we conduct a sensitivity analysis for storage of H$_2$ and electricity to evaluate the influence of the storage system. The results are illustrated in Fig. S8 in the ESI,† Section S5 for the
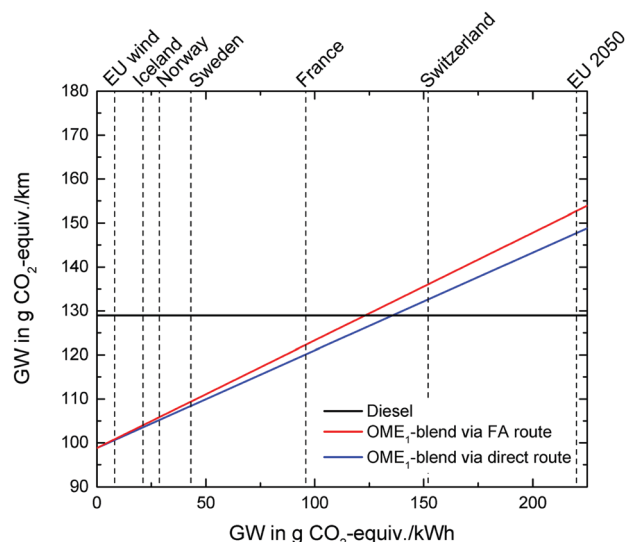

Fig. 8 Sensitivity analysis of the cradle-to-grave global warming (GW) impact of the OME$_1$-blend and diesel fuel as a function of the GW impact of the electricity supply. The dashed vertical lines represent the GW impact of various national electricity grid mixes and a forecast average grid mix for Europe in 2050. CO$_2$ is supplied from a biogas plant.

GW impact and the emissions of NOx and soot. For both the GW impact and the NOx emissions, the increase is lower than 1%. For soot emissions, the increase is lower than 3%.

5 Conclusions

Oxymethylene ethers (OMEs) are a promising class of CO_2-based fuels. Our comparative Life Cycle Assessment (LCA) of OME_1-blends and fossil diesel shows that OME_1-blends have the potential to substantially reduce environmental impacts from cradle-to-grave. To our knowledge, this LCA represents the first comprehensive environmental assessment of OME fuels in the public literature.

For our best-case scenario, the performance of OME_1 is even close to an ideal blending component, and reduces both global warming impacts and fossil depletion almost proportional to the amount of diesel fuel replaced. These environmental benefits depend strongly on the supply processes for the inputs to the OME_1 production process. Most importantly, benefits compared to diesel fuel can only be achieved if the electricity used for electrolysis is obtained from sources with a low GW impact and fossil cumulated energy demand (CED) since the OME_1-blend almost doubles the total CED. Suitable electricity sources include renewable energies and grid mixes with a large share of renewable or nuclear electricity. Such electricity grid mixes are available already today, *e.g.*, in Scandinavian countries. OME_1-blends would thus enable the integration of renewable energy into the existing transportation sector.

Emissions of NOx and soot are even reduced more strongly by the OME_1-blends. For these emissions, OME_1 acts synergistically: it reduces impacts beyond the emissions caused by the amount of diesel fuel replaced. This finding highlights the potential to design synthetic fuels which reduce harmful emissions from internal combustion engines.

For the production of OME_1, the formation of OME_1 from CO_2-based methanol and hydrogen (H_2) *via* formaldehyde has practically the same environmental impacts as the novel direct synthesis of OME_1 from methanol, H_2 and CO_2. However, due to a lower hydrogen demand, the direct route is less sensitive to the electricity sources employed. Fundamentally, the direct route has a higher exergetic efficiency indicating its thermodynamic advantage. Furthermore, the direct route requires only one reactor and possibly less heat exchangers and separation equipment, while the size of the methanol plant also could be reduced. These advantages indicate that more direct transformation pathways have the potential to improve overall efficiency. OME_1-blends could be an environmentally beneficial alternative to fossil diesel fuel. Their potential as a drop-in fuel candidate should be further explored *e.g.* by analyzing their impact on the distribution infrastructure. Linked to the transition towards renewable energy, OME_1-blends would allow the negative impacts of transportation on both human health and the environment to be reduced.

Conflicts of interest

There are no conflicts to declare.

Acknowledgements

References

1 Intergovernmental Panel on Climate Change (IPCC), *Climate Change 2014 Mitigation of Climate Change. Working Group III Contribution to the Fifth Assessment Report of the Intergovernmental Panel on Climate Change* 5, New York, 2014.
2 M. Hauschild and M. Huijbregts, *Life Cycle Impact Assessment*, Springer, Dordrecht Heidelberg New York London, 2015.
3 European Commission, eurostat, available at: http://ec.europa.eu/eurostat/home, accessed 2017.
4 J. Gieseke and G.-J. Gerbrandy, *On the inquiry into emission measurements in the automotive sector. Chapter 2: technical background*. Working Document No. 2, Committee of Inquiry into Emission Measurements in the Automotive Sector, 2016.
5 J. Klankermayer, S. Wesselbaum, K. Beydoun and W. Leitner, *Angew. Chem., Int. Ed.*, 2016, **55**, 7296–7343.
6 J. Klankermayer and W. Leitner, *Philos. Trans. R. Soc., A*, 2016, **374**, 20150315.
7 P. Markewitz, W. Kuckshinrichs, W. Leitner, J. Linssen, P. Zapp, R. Bongartz, A. Schreiber and T. E. Müller, *Energy Environ. Sci.*, 2012, **5**, 7281–7305.
8 R. Schlögl, *Angew. Chem., Int. Ed.*, 2015, **54**, 4436–4439.
9 G. Centi, E. A. Quadrelli and S. Perathoner, *Energy Environ. Sci.*, 2013, **6**, 1711–1731.
10 M. Matzen and Y. Demirel, *J. Cleaner Prod.*, 2016, **139**, 1068–1077.
11 G. Reiter and J. Lindorfer, *Int. J. Life Cycle Assess.*, 2015, **20**, 477–489.
12 A. Sternberg and A. Bardow, *Energy Environ. Sci.*, 2015, **8**, 389–400.
13 C. van der Giesen, R. Kleijn and G. J. Kramer, *Environ. Sci. Technol.*, 2014, **48**, 7111–7121.
14 D. Connolly, B. V. Mathiesen and I. Ridjan, *Energy*, 2014, **73**, 110–125.
15 N. von der Assen, L. J. Müller, A. Steingrube, P. Voll and A. Bardow, *Environ. Sci. Technol.*, 2016, **50**, 1093–1101.
16 W. Leitner, J. Klankermayer, S. Pischinger, H. Pitsch and K. Kohse-Höinghaus, *Angew. Chem., Int. Ed.*, 2017, **20**, 5412–5452.
17 G. A. Olah, A. Goeppert and G. K. S. Prakash, *Beyond Oil and Gas: The Methanol Economy*, Wiley-VCH, Weinheim, 2nd edn, 2009.

342 | *Energy Environ. Sci.*, 2018, **11**, 331–343

This journal is © The Royal Society of Chemistry 2018

18 F. Asinger, *Methanol—Chemie- und Energierohstoff*, Springer, Berlin Heidelberg, 1986.

19 *Methanol: the basic chemical and energy feedstock of the future: asinger's vision today*, ed. M. Bertau, H. Offermanns, L. Pass, F. Schmidt and H.-J. Wernicke, Springer-Verlag, Berlin/ Heidelberg, 2014.

20 W. Cho, T. Song, A. Mitsos, J. T. McKinnon, G. H. Ko, J. E. Tolsma, D. Denholm and T. Park, *Catal. Today*, 2009, **139**, 261–267.

21 I. Dimitriou, P. Garcia-Gutierrez, R. H. Elder, R. M. Cuellar-Franca, A. Azapagic and R. W. K. Allen, *Energy Environ. Sci.*, 2015, **8**, 1775–1789.

22 W. A. Kopp, L. C. Kröger, M. Döntgen, S. Jacobs, U. Burke, H. J. Curran, K. A. Heufer and K. Leonhard, *Combust. Flame*, 2017, DOI: 10.1016/j.combustflame.2016.12.021.

23 A. Balazs, M. Podworny, M. Schmitt, A. Feiling, C. Beidl, C. von Pyschow, E. Jacob and W. Maus, in *Internationaler Motorenkongress 2015. Mit Nutzfahrzeugmotoren-Spezial*, ed. J. Liebl and C. Beidl, *Springer Vieweg*, Wiesbaden, 2015, pp. 261–284.

24 J. Burger, Dissertation, Kaiserslautern University of Technology, 2012.

25 M. Härtl, P. Seidenspinner, E. Jacob and G. Wachtmeister, *Fuel*, 2015, **153**, 328–335.

26 L. Lautenschütz, D. Oestreich, P. Seidenspinner, U. Arnold, E. Dinjus and J. Sauer, *Fuel*, 2016, **173**, 129–137.

27 M. Münz, A. Feiling, C. Beidl, M. Härtl, D. Pélerin and G. Wachtmeister, in *Internationaler Motorenkongress 2016: Mit Konferenz Nfz-Motorentechnologie*, ed. J. Liebl and C. Beidl, *Springer Fachmedien*, Wiesbaden, 2016, pp. 537–553.

28 N. Schmitz, F. Homberg, J. Berje, J. Burger and H. Hasse, *Ind. Eng. Chem. Res.*, 2015, **54**, 6409–6417.

29 M. Ouda, G. Yarce, R. J. White, M. Hadrich, D. Himmel, A. Schaadt, H. Klein, E. Jacob and I. Krossing, *React. Chem. Eng.*, 2017, **2**, 50–59.

30 J. O. Drunsel, Dissertation, Technischen Universität Kaiserslautern, 2012.

31 J.-O. Weidert, J. Burger, M. Renner, S. Blagov and H. Hasse, *Ind. Eng. Chem. Res.*, 2017, **56**, 575–582.

32 B. G. Schieweck and J. Klankermayer, *Angew. Chem., Int. Ed.*, 2017, **56**, 10854–10857.

33 K. Thenert, K. Beydoun, J. Wiesenthal, W. Leitner and J. Klankermayer, *Angew. Chem., Int. Ed.*, 2016, **55**, 12266–12269.

34 F. Møller, E. Slentø and P. Frederiksen, *Biomass Bioenergy*, 2014, **60**, 41–49.

35 J. L. Sullivan, R. E. Baker, B. A. Boyer, R. H. Hammerle, T. E. Kenney, L. Muniz and T. J. Wallington, *Environ. Sci. Technol.*, 2004, **38**, 3217–3223.

36 I. T. Herrmann, M. Lundberg-Jensen, A. Jørgensen, T. Stidsen, H. Spliid and M. Hauschild, *Int. J. Life Cycle Assess.*, 2014, **19**, 194–205.

37 ISO – International Organization for Standardization, *ISO 14040. Environmental Management: Life Cycle Assessment: Principles and Framework*, 2006.

38 ISO – International Organization for Standardization, *ISO 14044. Environmental management—life cycle assessment— requirements and guidelines*, 2006.

39 N. von der Assen, J. Jung and A. Bardow, *Energy Environ. Sci.*, 2013, **6**, 2721–2734.

40 N. von der Assen, P. Voll, M. Peters and A. Bardow, *Chem. Soc. Rev.*, 2014, **43**, 7982–7994.

41 European Commission – Joint Research Centre – Institute of Environment and Sustainability, *International Reference Life Cycle Data System (ILCD) Handbook. Recommendations for Life Cycle Impact Assessment in the European context from the European Commission*, Publications Office of the European Union, Luxembourg, 2011.

42 R. Frischknecht, R. Heijungs and P. Hofstetter, *Int. J. Life Cycle Assess.*, 1998, **5**, 266–272.

43 G. Reuss, W. Disteldorf, A. O. Gamer and A. Hilt, Formaldehyde, *Ullmann's Encyclopedia or Industrial Chemistry*, Wiley-VCH, Weinheim, Germany, 2012, pp. 735–768.

44 H. Sperber, *Chem. Ing. Tech.*, 1969, **41**, 962–966.

45 D. Bongartz, L. Doré, K. Eichler, T. Grube, B. Heuser, L. E. Hombach, M. Robinius, S. Pischinger, D. Stolten, G. Walther and A. Mitsos, in preparation.

46 J. Scheffczyk, C. Redepenning, C. M. Jens, B. Winter, K. Leonhard, W. Marquardt and A. Bardow, *Chem. Eng. Res. Des.*, 2016, **115**(Part B), 433–442.

47 A. Godula-Jopek, *Hydrogen Production: by Electrolysis*, Wiley-VCH Verlag, Weinheim, 2015.

48 Swiss Centre for Life Cycle Inventories, *ecoinvent Data V 3.3*, 2016.

49 M. Götz, J. Lefebvre, F. Mörs, A. McDaniel Koch, F. Graf, S. Bajohr, R. Reimert and T. Kolb, *Renewable Energy*, 2016, **85**, 1371–1390.

50 S. Schiebahn, T. Grube, M. Robinius, V. Tietze, B. Kumar and D. Stolten, *Int. J. Hydrogen Energy*, 2015, **40**, 4285–4294.

51 A. Sternberg and A. Bardow, *ACS Sustainable Chem. Eng.*, 2016, **4**, 4156–4165.

52 Q. Zhao, E. Leonhardt, C. MacConnell, C. Frear and S. Chen, *Purification technologies for biogas generated by anaerobic digestion*, 2010.

53 European Commission, *EU energy, transport and GHG emissions Trends to 2050. Reference scenario 2013*, Luxembourg.

54 *GaBi 7.3.3. Software-System and Database for Life Cycle Engineering*, thinkstep AG, Leinfelden-Echterdingen, Germany, 2017.

55 M. Mori, M. Jensterle, T. Mržljak and B. Drobnič, *Int. J. Life Cycle Assess.*, 2014, **19**, 1810–1822.

56 G. Majeau-Bettez, T. R. Hawkins and A. H. Strømman, *Environ. Sci. Technol.*, 2011, **45**, 4548–4554.

57 C. Julien, A. Mauger, A. Vijh and K. Zaghib, *Lithium Batteries. Science and Technology*, Springer, Cham Heidelberg New York Dordrecht London, 2016.

58 A. Omari, B. Heuser and S. Pischinger, *Fuel*, 2017, **209**, 232–237.

59 *ASCMO. Data-based Modeling and Model-based Calibration*, ETAS, 2016.

60 T. V. Johnson, *SAE Int. J. Engines*, 2015, **8**, 1152–1167.

61 K. I. Svensson, M. J. Richards, A. J. Mackrory and D. R. Tree, *SAE Technical Paper*, SAE International, 2005.

62 *Commission Regulation (EC) No 692/2008 as regards emissions from light passenger and commercial vehicles (Euro 6)*, 2012.

This journal is © The Royal Society of Chemistry 2018

Energy Environ. Sci., 2018, **11**, 331–343 | 343